

Scientific Paper

Doi: <http://dx.doi.org/10.1590/1809-4430-Eng.Agric.v43n5e20230046/2023>

DESIGN AND EXPERIMENT OF A COMBINED TYPE SPATIALLY LAYERED PROPORTIONAL FERTILIZATION DEVICE

Hang Li^{1,2}, Xin Lin^{1,2}, Jin He^{1,2*}, Caiyun Lu^{1,2}, Wenchao Yang^{1,2}

^{1,2*}Corresponding author. College of Engineering, China Agricultural University/Beijing, China.

Scientific Observing and Experiment Station of Arable Land Conservation (North Hebei), Ministry of Agricultural and Rural Affairs/Beijing, China.

E-mail: hejin@cau.edu.cn | ORCID ID: <https://orcid.org/0000-0001-5126-3220>

KEYWORDS

wheat, layered fertilization device, structure optimization, element distinct method, response surface experiment.

ABSTRACT

To solve the problems of low efficiency, poor fertilizer application, and low fertilizer utilization rate of existing wheat layered fertilization devices (LFD). This paper proposed a layered fertilization mode combining shallow fertilizer application based on rotary tillage and middle/deep fertilizer application of layered fertilizer shovel (LFS), and designed a combined spatial layered fertilization device with a fixed proportion. A discrete element simulation model consisting of soil, LFS and fertilizer was established. Taking the variation coefficients of fertilization amount as the evaluation indicator and changing the sidewall deflection angle, rear inclination angle, upper channel length of LFS, a three-factor three-level quadratic rotational orthogonal experiment was carried out. The optimal parameter combination was obtained: the deflection angle was 9.5°, the inclination angle was 57°, and the channel length was 280 mm. The corresponding variation coefficients of fertilizer application depth were 4.55%, 8.44%, and 6.93% while working stably under the optimal combination, which is consistent with the simulation results. The results showed that LFD can apply fertilizer underground in three layers: 0~10, 15, and 20 cm, with the proportion of shallow, middle, and deep fertilizers being 30%, 35%, and 35%, which can meet the agronomic requirements for winter wheat growth.

INTRODUCTION

Wheat is one of the most important sources of food and nutrition for human beings, and more than one-third of the world's population relies on wheat as their staple food (Mottaleb et al., 2023). Ensuring the high and stable yield of wheat is significant to maintain grain safety. Wheat has a long growing season and requires amounts of nutrients (McLaughlin & Kinzelbach, 2015). Appropriate fertilization can effectively improve the yield and quality of wheat. Currently, the fertilization of wheat method is still dominated by the traditional fertilization mode. It mainly adopts manual staged spreading or one-time fertilization during sowing, which costs a large amount of fertilizer and has a low fertilizer utilization rate. One-time fertilization during sowing can easily cause wheat to burn early, and the nutrient supply is insufficient in the later stage (Zhan et al., 2011; Zeng et al., 2008). The traditional

fertilization mode is difficult to meet the developing requirements of modern agriculture (Yang et al., 2020b). Root growth is essential for wheat growth and metabolism (Shen et al., 2013). The root growth of wheat is fertilizer-oriented, and the growth of wheat is closely related to the location of fertilizer application. Wu et al. (2022) found that deep fertilization increased the antioxidant defense and photosynthetic capacity of maize leaves, which in turn increased maize yield. Li et al. (2021a) found that deep nitrogen fertilizer application can effectively increase leaf area during rice tasseling, improve grain yield, and reduce greenhouse gas emissions. Rational subsoiling and deep fertilizer application can promote crop root growth in the deep soil layer, add wheat's deep soil root biomass, and improve water utilization. However, just deep application can cause insufficient nutrient supply in the early stage of the crop, resulting in wheat yield reduction (Li et al., 2021b; Yin et al., 2021).

¹ College of Engineering, China Agricultural University/Beijing, China.

² Scientific Observing and Experiment Station of Arable Land Conservation (North Hebei), Ministry of Agricultural and Rural Affairs/Beijing, China.

Area Editor: Murilo Mesquita Baesso

Received in: 3-19-2023

Accepted in: 10-17-2023

In order to improve fertilizer utilization and application operation efficiency, relevant scholars have proposed layered fertilizer application technology. Liu et al. (2023) conducted a two-year agronomic experiment on winter wheat in the North China Plain. It was found that single surface fertilization or deep fertilization could not meet the nutritional requirements of winter wheat. Layered fertilization of winter wheat can promote the wheat root system's proliferation and improve winter wheat yield. Layered fertilization is to apply fertilizer required by the whole growth cycle of crops to different depths of the soil at one time by layered fertilization device. It can reduce environmental pollution and seed burning, improve operation efficiency and fertilizer utilization, ensure nutrient supply, and increase crop yield (Wang et al., 2016a). Applying the fertilizer needed by the crop to the required depth precisely according to the agronomic requirements of crop growth is the key to realizing the layered fertilization technology. For this reason, relevant experts and scholars have designed a series of LFDs according to the agronomic requirements of different crops. Zuo et al. (2022) had designed a spatially layered proportional fertilizer application device for summer corn, which could achieve fertilization in three layers at a ratio of 3:3:4 within 80-250mm. Wang et al. (2022) designed a maize precision strip-hole layered fertilization subsoiler. Du et al. (2022) designed a fertilizer point-applied device in root-zone that could apply the required fertilizer to the roots in two layers. Zhu et al. (2018) designed a layered application device for winter wheat base fertilizer based on rotary tillage and recovering soil. It used a rotary tiller and a fertilizer delivery pipe to apply fertilizer in layers to the required depth. The research of related experts on LFDs is still in the experimental stage, mainly focusing on the research on LFDs for corn. At present, the wheat-LFDs can only apply fertilizer in two layers and only involves a certain aspect of limited depth or

fixed ratio fertilizer application. The single-function wheat-LFDs have low efficiency, poor fertilization effect, and low fertilizer utilization rate, which makes it difficult to meet the agronomic requirements of wheat growth. To improve fertilizer utilization and winter wheat yield, according to the agronomic requirements of winter wheat fertilization, there is an urgent need to develop a fixed-ratio quantitative LFD for winter wheat.

Given the above problems, the effect of fixed proportion fertilization, stratification effect and congestion reduction should be considered. This paper proposed a layered fertilization mode combining shallow fertilizer application and middle/deep fertilizer application based on rotary tillage and LFS, respectively. A combined spatial LFD with a fixed proportion is designed. The discrete element method (DEM) was used to simulate the operation process of the LFS, and field tests verified the performance of the LFD.

MATERIAL AND METHODS

Overall Structure and Working Principle of Layered Fertilization System

The layered fertilization system mainly includes LFD and fertilizer supply device (Fig. 1). The LFD is critical in realizing the layered application of fertilizers. It mainly comprises a shallow fertilizer application mechanism and LFSs. The shallow fertilizer application mechanism includes a rotary tillage device and fertilizer guide plates. The fertilizer supply device is divided into two sets, namely the shallow fertilizer application mechanism and the LFS. It mainly includes two fertilizer tanks, fertilizer application motors, fertilizer feeder, and fertilizer supply tubes. The LFS is critical in realizing the layered application of middle and deep layer fertilizer. It is mainly composed of a sub-soiling shovel and a fertilizer channel (Fig. 2a).

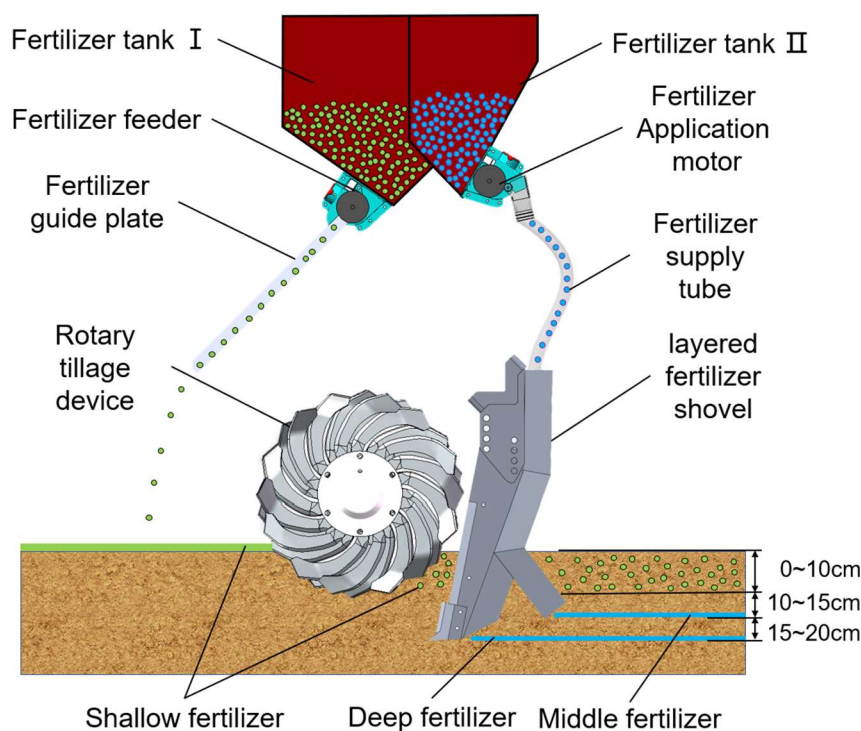


FIGURE 1. Structure diagram of the layered fertilization system.

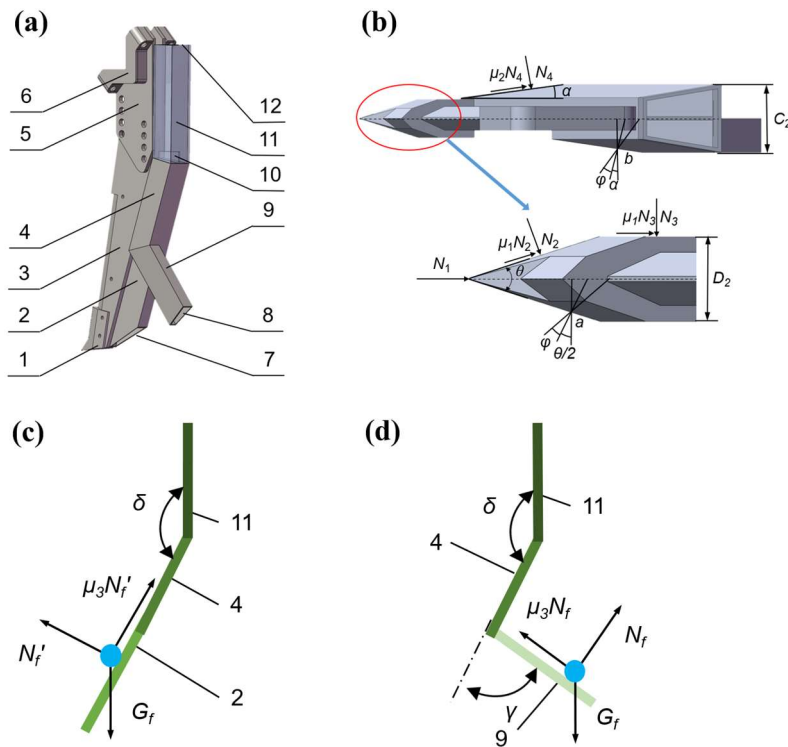


FIGURE 2. Structure and force analysis diagram of the LFS: 1, shovel tip; 2, deep fertilizer channel; 3, shovel handle; 4, lower fertilization channel; 5, support plate; 6, mounting block; 7, deep fertilizer outlet; 8, middle fertilizer outlet; 9, middle fertilizer channel; 10, divider; 11, upper channel; 12, fertilizer inlet.

According to the layered fertilization ratio of wheat in the Huang-Huai-Hai area, the speed of the fertilization motor is adjusted so that the ratio of shallow fertilizer to middle and deep fertilizer is 3:7. When the system is working, the fertilizer application motor drives the fertilizer feeder at a certain speed to discharge the shallow fertilizer from the fertilizer tank I and spread it into the ground in front of the machine. The rotary tillage device mixes up the shallow fertilizer and soil at a depth of 0 to 10 cm underground. Middle and deep fertilizer is drained from tank II. With the help of the divider, the fertilizer is evenly distributed to both sides and falls into the middle and deep fertilizer channels,

respectively. The final system can apply fertilizer underground in three layers 0~10, 15, and 20 cm underground, with the proportion of shallow, middle, and deep fertilizers being 30%, 35%, and 35%, respectively (Yang et al., 2020a).

Structural Design of LFS

The basic parameters of the LFS are shown in Figure 3. The sub-soiling shovel is a straight-pointed trenching shovel (Wang et al., 2016b). The main dimensions are shown in Table 1 (Ucgul et al., 2015; Zhang et al., 2021). Force analysis of the LFS is performed to determine the main parameters that influence its working performance.

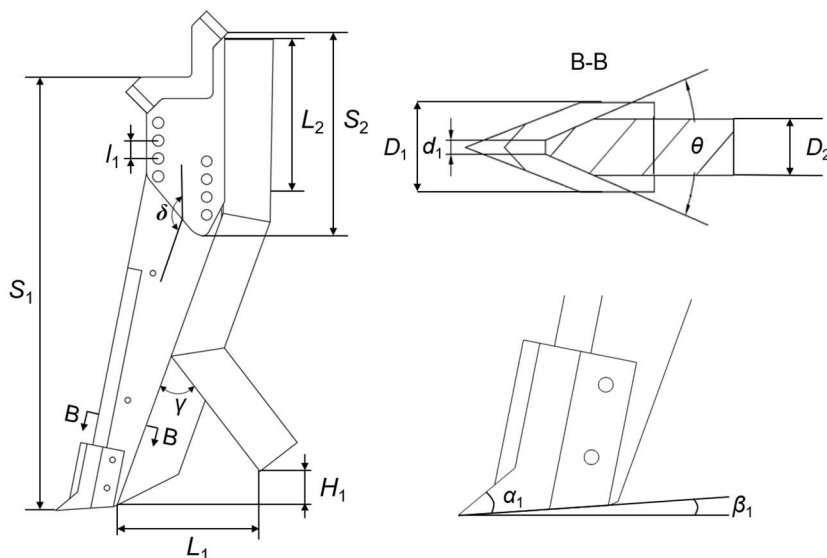


FIGURE 3. Basic parameters of the LFS.

TABLE 1. Geometric information of the LFS.

Parameter	Definition	Value
S_1 (mm)	Overall length	600
S_2 (mm)	Support plate width	250
l_1 (mm)	Distance of adjacent holes	25
C_1 (mm)	Upper side of the trapezoid	30
C_2 (mm)	Lower bottom edge of the trapezoid	60
D_1 (mm)	Shovel tip thickness	40
D_2 (mm)	Shovel handle thickness	30
d_1 (mm)	Width of the facing surface	5
δ (°)	Installation angle	160
θ (°)	Facing the soil angle	40
α_1 (°)	Shovel tip into the soil angle	35
β_1 (°)	Angle into the soil gap	8
H_1 (mm)	Distance between middle and deep fertilizer outlets.	50

Force analysis of LFS touching-soil components

The front width of the fertilizer channel is the same as the thickness of the shovel handle. Therefore, the sides of the sub-soiling shovel and fertilizer channel can be simplified as a whole force analysis. The force analysis of the top view of the LFS is shown in Figure 2b. The working resistance F_N of the LFS during operation can be expressed as:

$$F_N = N_1 + 2(N_2 \sin \frac{\theta}{2} + \mu_1 N_2 \cos \frac{\theta}{2} + \mu_1 N_3 + N_4 \sin \alpha + \mu_2 N_4 \cos \alpha) \quad (1)$$

Where:

θ is the angle of the handle;

α is the sidewall deflection angle;

μ_1 is the frictional coefficient between soil and shovel;

μ_2 is the frictional coefficient between soil and channel;

N_1 is the soil resistance in the vertical direction of the shovel handle, N;

N_2 is the normal component force of the soil resistance on the side of the shovel handle, N;

N_3 is the pressure of the soil on the side of the shovel handle, N, and

N_4 is the normal component force of the soil resistance of the fertilizer channel, N.

Analysis of soil movement trajectory of LFS

After the LFS cuts through the soil, the soil particles are broken and squeezed by the LFS. Its trajectory is in the same direction as the extrusion force it is subjected. Taking the soil particles at point "a" as an example, with the influence of the slope and surface friction of the device, the soil particles moving to point "a" have deviated (Fig. 2b). Its maximum offset L_k can be expressed as:

$$L_k = \frac{D_2}{2 \cos(\frac{\theta}{2} + \varphi)} \quad (2)$$

Where:

D_2 is the shovel handle width, mm; and φ is the friction angle between soil and LFS.

Similarly, the maximum offset of soil particles at the fertilizer channel is at the end of the fertilizer channel, L_k' can be expressed as:

$$L_k' = \frac{C_2}{2 \cos(\alpha + \varphi)} \quad (3)$$

Where:

C_2 is the back-end width of the fertilizer channel, mm.

The averaged soil shape change at the fertilizer channel can be expressed as:

$$\bar{L}_k = \frac{L_k + L_k'}{2} = \frac{D_2}{4 \cos(\frac{\theta}{2} + \varphi)} + \frac{C_2}{4 \cos(\alpha + \varphi)} \quad (4)$$

Analysis of fertilizer particle movement in the fertilizer channel

After leaving the fertilizer supply tube, the fertilizer granules fall into the fertilizer channel. The motion of the fertilizer particles in the fertilizer channel can be simplified as an oblique throwing motion. Fertilizer granules are subject to the action of gravity G_f and air resistance F_f (Cool et al., 2014). The equation can be expressed as:

$$m_f \frac{dv}{dt} = G_f + F_f \quad (5)$$

Of which:

$$F_f = -C_a A V_f \frac{\rho_a}{2} |v_f| \quad (6)$$

$$G_f = m_f g \quad (7)$$

Where:

m_f is the mass of fertilizer granules, kg;

g is the acceleration of gravity, m/s²;

C_a is the air resistance coefficient, determined by the Reynolds number of the air (Dong et al., 2007);

A is the contact area, m²;

v_f is the velocity of particle motion, m/s;

ρ_a is the air density, kg/m³,

V_f is the volume of fertilizer granules, m³.

Since the angle between the deep fertilizer channel and the ground is significant, the fertilizer particles can be discharged entirely by gravity. Therefore, the force on fertilizer particles in the middle fertilizer channel is mainly analyzed (Fig. 2c and 2d). The force equation for the fertilizer granules in the middle fertilizer channel is:

$$F_z = G_f \sin\left(\frac{3\pi}{2} - \delta - \gamma\right) - \mu_3 N_f \quad (8)$$

$$N_f = G_f \cos\left(\frac{3\pi}{2} - \delta - \gamma\right) \quad (9)$$

Combine eqs. (7), (8) and (9):

$$F_z = m_f g \sin\left(\frac{3\pi}{2} - \delta - \gamma\right) - \mu_3 m_f g \cos\left(\frac{3\pi}{2} - \delta - \gamma\right) \quad (10)$$

Where:

F_z is the combined force on the fertilizer particles along the slope direction;

G_f is the gravitational force on the fertilizer particles;

δ is the installation angle of the sub-soiling shovel;

γ is the posterior inclination angle of the middle fertilizer channel;

μ_3 is the coefficient of friction between the fertilizer particles and the inner tube wall of the fertilizer channel,

N_f is the support force for fertilizer particles.

Construction of Simulation Model

The three-dimensional model of the LFS was created by SolidWorks and simulated by EDEM software. The Hertz-Mindlin (no-slip) model is applied to the contact between soil and fertilizer, fertilizer and fertilizer, and fertilizer and mechanism. The Hertz-Mindlin bonding contact model was used for soil particles in the trough (Tang et al., 2020). The soil particles were spheres with a diameter of 10 mm. The fertilizer could roughly be simplified to spherical particles with a diameter of 3.28 mm. A soil trough was built with dimensions ($L \times W \times H$) of 2000 mm \times 500 mm \times 400 mm, filled with soil particles. By reviewing the literature, the contact parameters between the particles were determined, as shown in Table 2, and the model parameters of fertilizer particles, soil particles, and the LFD, are shown in Table 3 (Zuo et al., 2022; Wang et al., 2022; Yang et al., 2021). A particle factory at the fertilizer channel's upper position was created to mimic the fertilizer's falling from the initial state into the fertilizer channel through the fertilizer supply tube. The forward speed of the LFS mimics the forward speed during normal fertilizer application and was set to 1 m/s. The particle factory and the LFS moved forward at the same speed (Fig. 4), and the total simulation time was 3 s.

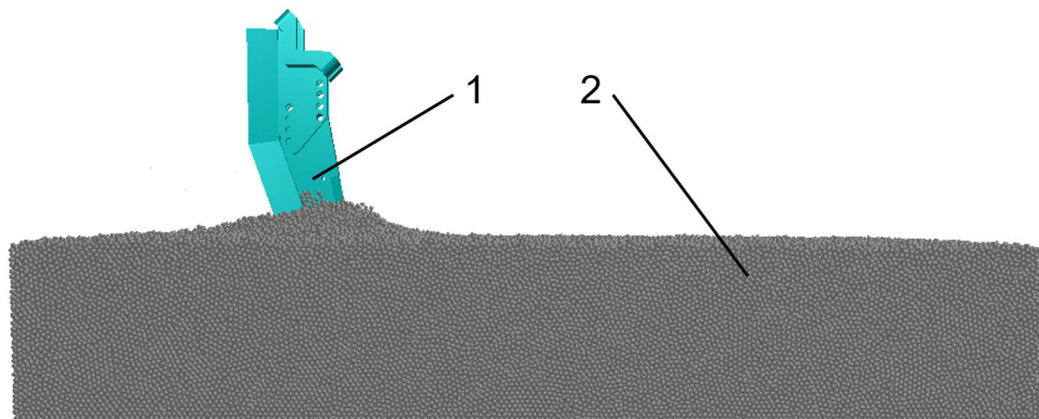


FIGURE 4. EDEM simulation model: 1, LFS; 2, Soil troughs.

TABLE 2. Contact parameters between particles.

Materials	Coefficient of Restitution	Coefficient of Static Friction	Coefficient of Dynamic Friction
Fertilizer-fertilizer	0.402	0.434	0.05
Fertilizer-soil	0.41	0.4	0.02
Soil-soil	0.6	0.33	0.17
Fertilizer-LFS	0.59	0.312	0.01
Soil -LFS	0.6	0.42	0.05

TABLE 3. Simulation parameters.

Materials	Poisson's Ratio	Density (kg/m ³)	Shear Modulus (Pa)
LFS	0.269	7890	7.0×10 ¹⁰
Fertilize	0.25	1490	2.9×10 ⁸
Soil	0.3	1925	1×10 ⁶

Single-factor test validation

The analysis showed that the main factors affecting the working quality of the LFS were: the sidewall deflection angle of the fertilizer channel (*A*), the rear inclination angle of the middle fertilizer channel (*B*), and the length of the upper channel (*C*). The values-range of the main factors was determined by pre-testing. The effect of fertilizer channel parameters on the stratification effect of fertilizer in the middle and deep layers was analyzed by a single-factor test. The feasibility of the range of values of the main factors was verified in the following sections.

TABLE 4. Experimental factors and levels.

Level	A/(°)	B/(°)	C/(mm)
-1	5	30	200
0	15	50	250
1	25	70	300

Field-Test Verification

In order to verify the optimized parameter combinations obtained from the simulation tests, the LFD was processed, and field performance tests were conducted. The test site is located in Shenze County, Shijiazhuang City, Hebei Province, at about 115°12'E and 38°11'N. It belongs to the Huang-Huai-Hai

Quadratic Regression Orthogonal Rotation Combination Design Simulation Experiment

The LFS was a critical component of the layered fertilization system. In order to investigate the effect of different parameters of the fertilizer channel on the operating quality of the LFS. The coefficient of variation of fertilizer application amount in each layer was used as the test index, and *A*, *B*, and *C* were the test factors. The three-factor three-level quadratic rotational orthogonal test was conducted. The ranges of levels of three factors were *A* (5°~25°), *B* (30°~70°), and *C* (200~300 mm). The coding of test factors is shown in Table 4.

wheat-corn two-cropping planting land a year. The front stubble crop was corn, with some stalks on the ground. The test was conducted with a lovol M1254 tractor with a rated power of 93 kW and a counterweight of 400 kg. The fertilizer chosen for the experiment was a compound fertilizer produced by SKF Ltd. The field test is shown in Figure 5.



FIGURE 5. Schematic diagram of the field operation of the LFD.

The LFS was tested for layered performance before the field test. For the convenience and accuracy of collecting data, fertilizer was collected at the fertilizer application port with a catch bag to test the distribution ratio of each layer of fertilizer (Fig. 6a). According to the specific requirements for fertilizer application devices in JB/T 8401.1-2007 (Rototill combine equipment - Rototill seed-cum-fertilizer drill), and GB/T 9478-2005 (Testing methods of sowing in lines), we use the application depth, application ratio, and variation coefficient of the shallow, middle, and deep fertilizers as evaluation indexes. The stability of the operational performance of the

LFD was experimentally studied under different application amounts (Hu et al., 2020). By sampling and testing the divided plots, it was determined that the amount of fertilizer required for different plots was divided into four classes, 525-600, 600-675, 675-750, and 750-825 kg/hm² (Meng et al., 2009). Before the test, the fertilizer discharge system's fertilizer application volume was calibrated to determine the machine's forward speed and discharge speed under different fertilizer application volumes. After the experiment, three collection points were randomly selected in each plot to measure the depth of each layer of fertilizer (Fig. 6b).

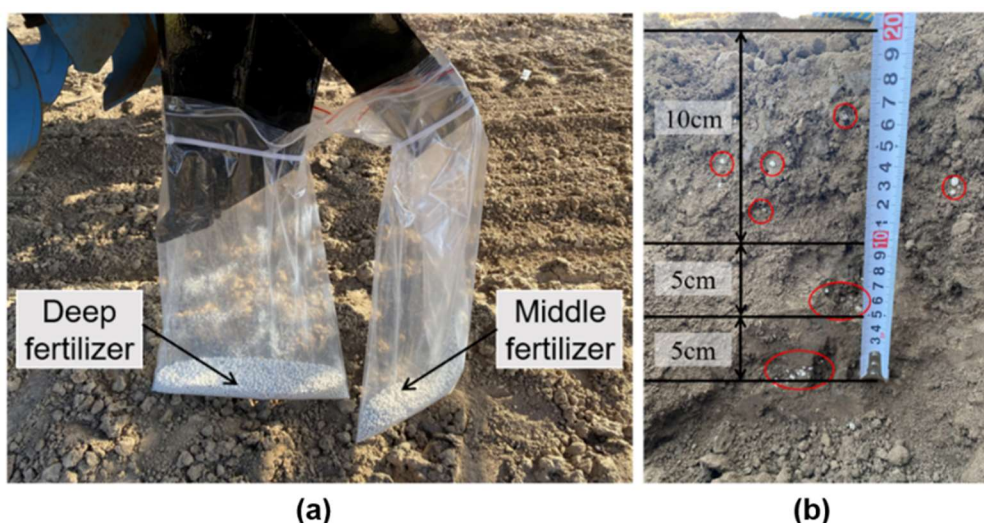


FIGURE 6. Fertilization effect in field.

RESULTS AND DISCUSSION

Analysis of the main factors affecting the LFS performance

From [eq. (1)], α is the main factor influencing the working resistance of the LFS. High α value is associated with high working resistance. A relatively small α value leads to insufficient fertilizer through the area, which will cause fertilizer blockage. It can influence the quality of layered

fertilization operations. From [eq. (4)], α is an essential factor affecting the amount of soil shape change at the fertilizer channel. The increase of soil deformation degree will influence the rate of soil returning, the effect of ditching, and the layered fertilization operation. From [eq. (10)], the combined force on the fertilizer particles along the inclined direction is influenced by the γ . Therefore, the change of the γ affects the falling motion of the fertilizer particles, which in turn affects the operation effect. The movement of fertilizer

particles is a continuous process. However, with each collision of fertilizer particles with the inner wall of the fertilizer channel and the change in the movement speed of fertilizer particles, the movement of fertilizer particles in the air will also change, affecting the uniformity of throwing. The fertilizer particles are not subjected to the external additional air force, so the most significant influence on the falling characteristics of the fertilizer particles is the collision between the fertilizer particles and the fertilizer channel and the longer movement time of the fertilizer particles within the upper part of the fertilizer channel, the more uniform its distribution within the fertilizer channel, and thus the upper channel length L_2 affects the proportional distribution of the fertilizer, thereby affecting the effect of the layered fertilizer application operation. The length L_2 is an important parameter that affects whether the fertilizer can fall evenly into the channels on both sides of the divider. The larger value of L_2 makes the more uniform movement of the fertilizer channel and the better stratification effect.

Single-Factor Analysis of the LFS Tests

From Figure 7a: the displacement of soil particles increased with the increase of A . It causes the late return of

soil, which affected stratified fertilization. However, when A is too small, fertilizer aggregation occurs in the fertilizer layer. It can also be seen in the fertilizer channel that fertilizer aggregation occurs in the trapezoidal narrow opening of the middle layer of the fertilizer channel, from which it can be seen that if A is too small, it will reduce the passable area of the fertilizer. It will be easier to be clogged.

From Figure 7b: a smaller B would make the middle layer fertilizer outlet closer to the deep layer fertilizer outlet, causing a late return to the soil and affecting the layering effect. When B was too large, it would make the combined force of fertilizer in the middle fertilizer channel along the channel direction smaller, and the fertilizer move longer. The fertilizer would discharge slower, causing fertilizer blockage.

From Figure 7c: The amount of fertilizer applied to the middle layer was significantly less than that to the deep layer when C was too small. With the increase of C , the layering effect of the two-layer fertilizer belt gradually became better. The length of C affected the movement of fertilizer in the application channel before it divided, resulting in uneven distribution of the ratio and ultimately affecting the effect of layered fertilization.

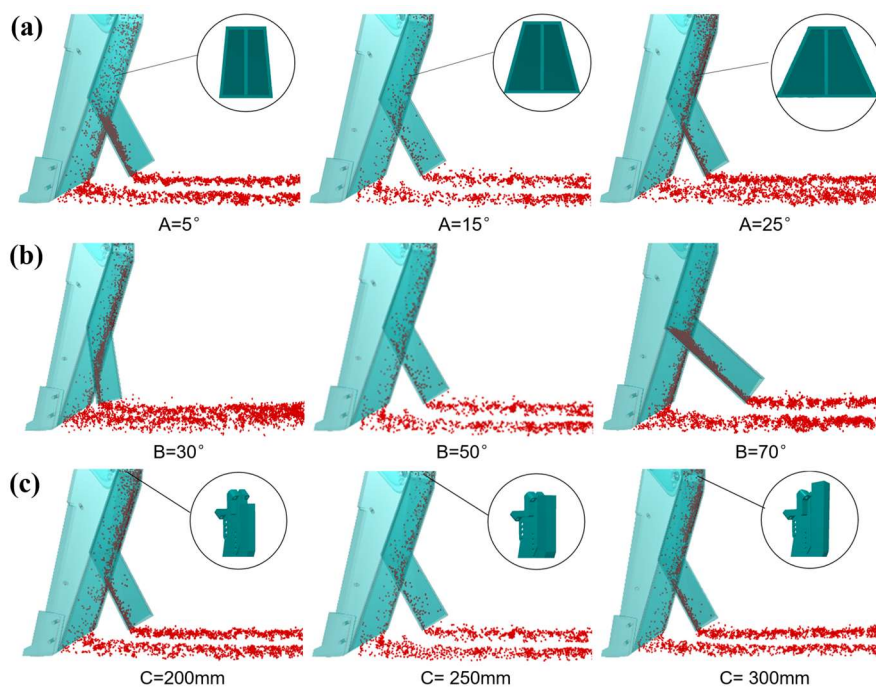


FIGURE 7. Stratification effect of the LFS under different parameters.

Through theoretical analysis and single-factor test, the value range of the critical parameters affecting the effect of LFS operation was determined: A was $5^\circ\sim 25^\circ$, B was $30^\circ\sim 70^\circ$, and C was 200~300 mm.

Test of Variance and Quadratic Regression Model Results and Analysis

Regression Model Construction

The simulation results are shown in Table 5. The experimental results were analyzed by quadratic regression

using Design-Expert and fitted with multiple regression. Mathematical relationships were obtained between the variation coefficient of the actual fertilizer application amount in the middle layer X_1 , the variation coefficient of the actual fertilizer application amount in the deep layer X_2 , the variation coefficient of fertilizer application difference X_3 , and A, B, C . The order of predominance of factors affecting X_1, X_2 and X_3 are all $A > B > C$. The non-significant terms in the ANOVA were removed, and the ANOVA was performed again. The model was analyzed to test for significance and interaction, and the analysis of variance is shown in Table 6.

TABLE 5. Test design and experimental data.

Test	A (°)	B (°)	C (mm)	X ₁ (%)	X ₂ (%)	X ₃ (%)
1	5	30	250	16.24	15.9	17.03
2	5	50	300	6.13	5.9	5.62
3	15	50	250	8.32	7.5	7.58
4	15	30	200	15.94	14.44	15.16
5	25	30	250	19.02	17.55	17.73
6	25	50	200	12.96	12.65	13.87
7	15	70	200	13.09	12.17	11.81
8	15	70	300	9.98	10.46	9.94
9	15	30	300	14.13	13.19	13.28
10	15	50	250	8.07	8.4	7.84
11	15	50	250	7.11	7.6	9.44
12	5	50	200	8.23	8.26	8.46
13	5	70	250	8.04	8.51	7.24
14	15	50	250	6.23	6.13	6.44
15	15	50	250	9.29	7.93	8.08
16	25	70	250	16.28	16.28	15.6
17	25	50	300	11.26	11.26	12.42

TABLE 6. Analysis of variance (after rejecting nonsignificant factors).

Indicator	Source of Variation	Sum of Squares	DF	Mean Square	F-Value	p-Value
X ₁	Mode	259.37/258.61	9/6	28.82/43.10	36.32/68.33	<0.0001***/<0.0001***
	A	56.02/56.02	1/1	56.02/56.02	70.61/88.81	<0.0001***/<0.0001***
	B	40.14/40.14	1/1	40.14/40.14	50.59/63.63	0.0002***/<0.0001***
	C	9.05/9.05	1/1	9.05/9.05	11.41/14.35	0.0118**/0.0036***
	AB	7.59/7.59	1/1	7.59/7.59	9.57/12.03	0.0175**/0.0060***
	A ²	14.54/14.78	1/1	14.54/14.78	18.32/23.43	0.0037***/0.0007***
	B ²	124.86/125.79	1/1	124.86/125.79	157.37/199.41	<0.0001***/<0.0001***
	Pure error	5.55/6.31	7/10	0.79/0.63		
X ₂	Mode	216.02/215.03	9/6	24.00/35.96	34.60/69.87	<0.0001***/<0.0001***
	A	44.98/44.98	1/1	44.98/44.98	64.83/87.41	<0.0001***/<0.0001***
	B	24.01/24.01	1/1	24.01/24.01	34.61/46.66	0.0006***/<0.0001***
	C	5.63/5.63	1/1	5.63/5.63	8.11/10.94	0.0248**/0.0079***
	AB	9.99/9.99	1/1	9.99/9.99	14.39/19.40	0.0068***/0.0013***
	A ²	17.27/17.30	1/1	17.27/17.30	24.89/33.62	0.0016***/0.0002***
	B ²	108.35/108.61	1/1	108.35/108.61	156.17/211.03	<0.0001***/<0.0001***
	Pure error	4.86/5.15	7/10	0.69/0.51		
X ₃	Mode	229.99/229.34	9/6	25.55/38.22	19.60/39.12	0.0004***/<0.0001***
	A	57.08/57.08	1/1	57.08/57.08	43.78/58.43	0.0003***/<0.0001***
	B	42.83/42.83	1/1	42.83/42.83	32.84/43.84	0.0007***/<0.0001***
	C	8.08/8.08	1/1	8.08/8.08	6.20/8.27	0.0416**/0.0165**
	AB	14.29/14.29	1/1	14.29/14.29	10.96/14.62	0.0129**/0.0034***
	A ²	17.21/17.44	1/1	17.21/17.44	13.20/17.85	0.0084***/0.0018***
	B ²	84.39/85.02	1/1	84.39/85.02	64.72/87.02	<0.0001***/<0.0001***
	Pure error	9.13/9.77	7/10	1.30/0.98		

The significance analysis of X_1 , X_2 and X_3 were obtained by analyzing and fitting the experiment results (Table 6). The regression equations are expressed:

$$X_1 = 58.14 - 0.64A - 1.58B - 0.02C + 0.01AB + 0.02A^2 + 0.01B^2 \tag{11}$$

$$X_2 = 54.65 - 0.77A - 1.47B - 0.02C + 0.01AB + 0.02A^2 + 0.01B^2 \tag{12}$$

$$X_3 = 54.46 - 0.81A - 1.37B - 0.02C + 0.01AB + 0.02A^2 + 0.01B^2 \tag{13}$$

The above regression equation were tested for the misfitting term, and the lack of fits were 0.7286、0.7715 and 0.6488, which were not significant. The fittings were well accepted. And there were significant quadratic relationships between the test indexes and the test factors.

Response Surface Analysis and Parameter Optimization

The test results were processed by Design-Expert

software. According to the established regression models of X_1 , X_2 , and X_3 . The response surface of the effect of interaction between factors on the test indexes was obtained and is shown in Fig. 8. For X_1 , X_2 and X_3 , the interaction of A and B affected the response surfaces. When B was fixed, X_1 , X_2 and X_3 decreased as A decreased, and the better range of A was $5^\circ \sim 15^\circ$. When A was fixed, B was parabolic with X_1 , X_2 and X_3 respectively, and the better range of B was $50^\circ \sim 64^\circ$.

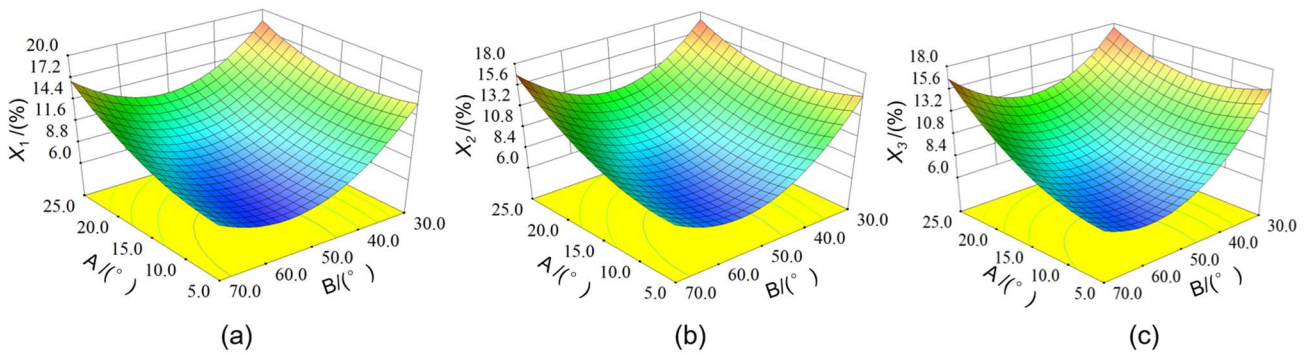


FIGURE 8. Response surface diagrams for double parameters.

In order to obtain the optimal structural parameters of the fertilizer channel, three regression models were solved for the optimization of the constraint target. The optimization constraints were selected according to the actual operation conditions. The objective and constraint functions were as follows:

$$\begin{cases} \min X_1(A, B, C) \\ \min X_2(A, B, C) \\ \min X_3(A, B, C) \\ \text{s.t.} \begin{cases} 5^\circ \leq A \leq 15^\circ \\ 50^\circ \leq B \leq 64^\circ \\ 200\text{mm} \leq C \leq 300\text{mm} \end{cases} \end{cases} \tag{14}$$

According to the constraints, the objective function was solved optimally to obtain multiple optimized parameter combinations and combined with the actual machining

situation. The better parameter combination was obtained: A was 9.5° , B was 57° , and C was 280 mm. At this point, the corresponding X_1 was 5.43% , X_2 was 5.74% , and X_3 was 6.49% .

Field-Test Results and Analysis

The data on the ratio of fertilizer application amount of deep-layer fertilizer to middle-layer fertilizer at different speeds is shown in Fig. 9a. The maximum variation coefficients of middle and deep fertilizers at different speeds were 8.76% and 8.49% . The relative errors of fertilizer fraction ratios were less than 5% . The device had good stability and met the design requirements. The stability of tillage depth could be used as a critical index to judge the fertilization performance of shallow fertilizer (Zhu et al., 2018). The average depths of tillage, middle and deep fertilizers were 103.86 mm, 139.7 mm, and 192.1 mm, the relative errors were 3.86% , 6.87% , and 3.95% , and the variation coefficients were 4.55% , 8.44% , and 6.93% , respectively (Fig. 9b).

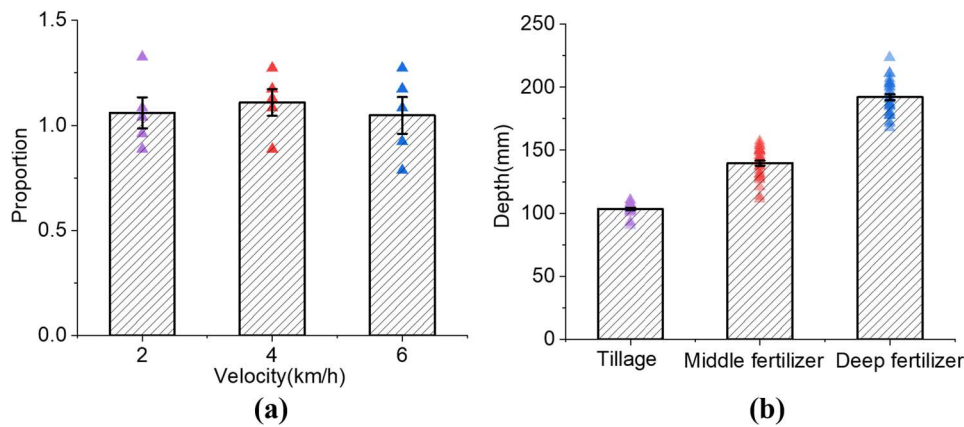


FIGURE 9. Results of performance.

The results were similar to the optimized results and could meet the agronomic requirements of winter wheat in China's Huang-Huai-Hai region. The average depth of tillage was slightly larger because of the errors in processing, installation and the low tractor's attached farm implement. However, from the perspective of layered fertilization performance requirements, it did not influence the effect of stratified fertilization. The average fertilization depths of middle and deep fertilizers were lower than the design expected. The main reason was that the soil returns slightly when the fertilizer fell, but the depth of fertilization did not fluctuate much, and its stability was within the design error range. The depth stability of shallow fertilizers compares slightly better with related studies, and the stability of mid-depth fertilizers compares slightly worse with related studies. Overall, it is not much different from the relevant studies and can meet the requirements of the relevant fertilizer application operational performance indicators (Zhu et al., 2018; Yang et al., 2020b). Therefore, the fertilization in the shallow, middle and deep layers could meet the requirements.

CONCLUSIONS

1. This article proposed a layered fertilization mode combining shallow fertilizer application based on rotary tillage and middle/deep fertilizer application of LFS, and designed a combined spatial layered fertilization device with a fixed proportion, which can apply fertilizer underground in three layers: 0~10, 15, and 20 cm, with the proportion of shallow, middle, and deep fertilizers being 30%, 35%, and 35%.
2. Through theoretical analysis and single-factor test, the value range of the critical parameters affecting the effect of LFS operation was determined: the sidewall deflection angle of the fertilizer channel A was 5°~25°, the rear inclination angle of the middle fertilizer channel B was 30°~70°, and the length of the upper channel C was 200~300 mm.
3. The experimental and influencing factors regression model was developed, and the experimental results were optimized and analyzed. The optimal parameter combination was obtained: A was 9.5°, B was 57°, and C was 280 mm. At this point, the corresponding variation coefficient of the actual fertilizer application amount in the middle layer was 5.43%, the actual fertilizer

application amount in the deep layer was 5.74%, and the fertilizer application difference was 6.49%.

4. The evaluation experiment of the LFD was conducted. The test results showed that the maximum variation coefficients of middle and deep fertilizers at different speeds were 8.76% and 8.49%. The variation coefficients of fertilizer application depth at different fertilizer application rates were 4.55%, 8.44%, and 6.93%, respectively. The results were similar to the optimized results and could meet the agronomic requirements of winter wheat in China's Huang-Huai-Hai region.

ACKNOWLEDGEMENTS

This research was funded by the China Agriculture Research System of MOF and MARA(Grant No.CARS-O3), the 2115 Talent Development Program of China Agricultural University and Chinese Universities Scientific Fund (Grant No.2021TC105), and Innovative Research Team in University of China(Grant No.IRT13039).

REFERENCES

- Cool S, Pieters J, Mertens KC, Hijazi B, Vangeyte J (2014) A simulation of the influence of spinning on the ballistic flight of spherical fertilizer grains. *Computers and Electronics in Agriculture* 105: 121-131. <https://doi.org/10.1016/j.compag.2014.04.014>
- Dong CY, Luan WL, Zhou ST, Zhang Q (2007) Analysis and application of model for solid particle movement in Newton fluid. *Journal of China University Petroleum* 31(6): 55-59.
- Du X, Liu CL, Jiang M, Yuan H (2022) Design and development of fertilizer point-applied device in root-zone. *Applied Engineering in Agriculture* 38(3): 559-571. <https://doi.org/10.13031/aea.14846>
- Hu J, He J, Wang Y, Wu YP, Chen C, Ren ZY Li XX, Shi SJ, Du YP, He PX (2020) Design and study on lightweight organic fertilizer distributor. *Computers and Electronics in Agriculture* 169: 105-149. <https://doi.org/10.1016/j.compag.2019.105149>
- Li GH, Cheng Q, Li L, Lu DL, Lu WP (2021b) N, P and K use efficiency and maize yield responses to fertilization modes and densities. *Journal of Integrative Agriculture* 20 (1): 78-86. [https://doi.org/10.1016/S2095-3119\(20\)63214-2](https://doi.org/10.1016/S2095-3119(20)63214-2)

- Li L, Hua T, Zhang MH, Fan PS, Ashraf U, Liu HD, Chen XF, Duan MY, Tang XR, Wang ZM, Zhang Z, Pan SG (2021a) Deep placement of nitrogen fertilizer increases rice yield and nitrogen use efficiency with fewer greenhouse gas emissions in a mechanical direct-seeded cropping system. *The Crop Journal* 9: 1386-1396. <https://doi.org/10.1016/j.cj.2020.12.011>
- Liu CH, Yan HH, Wang WY, Han RF, Li ZY, Lin X, Wang D (2023) Layered application of phosphate fertilizer increased winter wheat yield by promoting root proliferation and phosphorus accumulation. *Soil & Tillage Research* 225: 105546. <https://doi.org/10.1016/j.still.2022.105546>
- McLaughlin D, Kinzelbach W (2015) Food security and sustainable resource management. *Water Resources Research*; 51(7): 4966-4985. <https://doi.org/10.1002/2015WR017053>
- Meng Z, Zhao C, Liu H, Huang WQ, Fu WQ, Wang X (2009) Development and performance assessment of map-based variable rate granule application system. *Journal of Jiangsu University* 30(04): 338-342.
- Mottaleb KA, Kruseman G, Frijia A, Sonder K, Lopez-Ridaura S (2023) Projecting wheat demand in China and India for 2030 and 2050: implications for food security. *Frontiers in Nutrition* 9: 1077443. <https://doi.org/10.3389/fnut.2022.1077443>
- Shen YF, Li SQ, Shao MA (2013) Effects of spatial coupling of water and fertilizer applications on root growth characteristics and water use of winter wheat. *Journal of Plant Nutrition* 36(4): 515-528. <https://doi.org/10.1080/01904167.2012.717160>
- Tang H, Jiang YM, Wang JW, Wang JF, Zhou WQ (2020) Numerical analysis and performance optimization of a spiral fertilizer distributor in side deep fertilization of a paddy field. *Proceedings of the Institution of Mechanical Engineers Part C- Journal of Mechanical Engineering Science* 235(18): 3495-3505. <https://doi.org/10.1177/0954406220976158>
- Ucgul M, Fielke J, Saunders C (2015) Three dimensional discrete element modeling (DEM) of tillage: accounting for soil cohesion and adhesion. *Biosystems Engineering* 129: 298-306. <https://doi.org/10.1016/j.biosystemseng.2014.11.006>
- Wang QJ, Zhao HB, He J, Li HW, Chen WZ, Cao XJ, Rabi G (2016a) Design and experiment of blades-combined no and minimum-till wheat planter under controlled traffic farming system. *Transactions of the Chinese Society of Agricultural Engineering* 32(17): 12-17. <https://doi.org/10.11975/j.issn.1002-6819.2016.17.002>
- Wang WW, Song JL, Zhou GA, Quan LZ, Zhang CL, Chen LQ (2022) Development and numerical simulation of a precision strip-hole layered fertilization subsoiler while sowing maize. *Agriculture* 12(7): 938. <https://doi.org/10.3390/agriculture12070938>
- Wang YX, Liang ZJ, Cui T, Zhang DX, Qu Z, Yang L (2016b) Design and experiment of layered fertilization device for corn. *Transactions of the Chinese Society for Agricultural Machinery* 47(S1): 163-169. <https://doi.org/10.6041/j.issn.1000-1298.2016.S0.025>
- Wu P, Liu F, Chen GZ, Wang JY, Huang FY, Cai T, Zhang P, Jia ZK (2022) Can deep fertilizer application enhance maize productivity by delaying leaf senescence and decreasing nitrate residue levels? *Field Crops Research* 277: 108417. <https://doi.org/10.1016/j.fcr.2021.108417>
- Yang QL, Huang XY, Wang QJ, Li HW, Wang YB Wang LY (2020a) Structure optimization and experiment of corn layered fertilization device. *Transactions of the Chinese Society for Agricultural Machinery* 51(S1): 175-185. <https://doi.org/10.6041/j.issn.1000-1298.2020.S1.020>
- Yang QL, Li HW, He J, Lu CY, Wang YB, Wang QJ (2021) Design and experiment of layered deep fertilization device of different fertilizers based on pneumatic distribution. *Transactions of the Chinese Society for Agricultural Machinery* 52(10): 61-73. <https://doi.org/10.6041/j.issn.1000-1298.2021.10.006>
- Yang QL, Wang QJ, Li HW, He J, Lu CY, Yu CC, Lou SY, Wang YB (2020b) Development of layered fertilizer amount adjustment device of pneumatic centralized variable fertilizer system. *Transactions of the Chinese Society of Agricultural Engineering* 36(01): 1-10. <https://doi.org/10.11975/j.issn.1002-6819.2020.01.001>
- Yin BZ, Hu ZH, Wang YD, Zhao J, Pan ZH, Zhen WC (2021) Effects of optimized subsoiling tillage on field water conservation and summer maize (*Zea mays* L.) yield in the North China Plain. *Agricultural Water Management* 247: 106732. <https://doi.org/10.1016/j.agwat.2020.106732>
- Zeng SC, Su ZY, Chen BG, Chen BG, Wu QT Ouyang Y (2008) Nitrogen and phosphorus runoff losses from orchard soils in South China as affected by fertilization depths and rates. *Pedosphere* 18(1): 45-53. <https://doi.org/10.1590/1809-4430-Eng.Agric.v42n1e20210112/2022>
- Zhan X, Li TT, Han XR, Zou DB, Zuo R, Ye B (2011) Effects of nitrogen fertilization methods on yield, profit and nitrogen absorption and utilization of spring maize. *Plant Nutrition and Fertilizer Science* 17(04): 861-868.
- Zhang SW, Wang ZL, Wang L, Liu S, Zhang YJ, Miao H, Dai M, Liu SX (2021) Design and experimental study of ginkgo leaf picking device. *Proceedings of the Institution of Mechanical Engineers Part C-Journal of Mechanical Engineering Science* 235(24): 7353-7362. <https://doi.org/10.1177/09544062211023118>
- Zhu Q, Wu G, Chen L, Meng ZJ, Shi JT, Zhao CJ (2018) Design of stratified and depth-fixed application device of base-fertilizer for winter wheat based on soil-covering rotary tillage. *Transactions of the Chinese Society of Agricultural Engineering* 34(13): 18-26. <https://doi.org/10.11975/j.issn.1002-6819.2018.13.003>
- Zuo Z, Zhao JG, Yin BZ, Li LX, Jia HT, Zhang BC, Ma ZK, Hao JJ (2022) Optimized design and experiment of a spatially stratified proportional fertilizer application device for summer corn. *ACS Omega* 7(24): 20779-20790. <https://doi.org/10.1021/acsomega.2c01273>